Title
Effects of non-hydrostaticity and grain size on the pressure-induced phase transition of the CoCrFeMnNi high-entropy alloy

Journal
Journal of Applied Physics, 124(11)

ISSN
0021-8979

Authors
Zhang, Fei
Lou, Hongbo
Chen, Songyi
et al.

Publication Date
2018-09-21

DOI
10.1063/1.5046180

Peer reviewed

Journal of Applied Physics

Effects of non-hydrostaticity and grain size on the pressure-induced phase transition of the CoCrFeMnNi high-entropy alloy

Cite as: J. Appl. Phys. **124**, 115901 (2018); https://doi.org/10.1063/1.5046180
Submitted: 26 June 2018 . Accepted: 22 August 2018 . Published Online: 18 September 2018

Fei Zhang, Hongbo Lou, Songyi Chen, Xiehang Chen, Zhidan Zeng, Jinyuan Yan, Wuxin Zhao, Yuan Wu, Zhaoping Lu, and Qiaoshi Zeng

Effects of non-hydrostaticity and grain size on the pressure-induced phase transition of the CoCrFeMnNi high-entropy alloy

Fei Zhang,[1,2] Hongbo Lou,[2] Songyi Chen,[2] Xiehang Chen,[2] Zhidan Zeng,[2] Jinyuan Yan,[3,4] Wuxin Zhao,[1] Yuan Wu,[1] Zhaoping Lu,[1,a)] and Qiaoshi Zeng[2,5,a)]
[1]*State Key Laboratory for Advanced Metals and Materials, University of Science and Technology Beijing, Beijing 100083, People's Republic of China*
[2]*Center for High Pressure Science and Technology Advanced Research, Pudong, Shanghai 201203, People's Republic of China*
[3]*Advanced Light Source, Lawrence Berkeley National Laboratory, Berkeley, California 94720, USA*
[4]*Department of Earth and Planetary Sciences, University of California, Santa Cruz, Santa Cruz, California 95064, USA*
[5]*Jiangsu Key Laboratory of Advanced Metallic Materials, School of Materials Science and Engineering, Southeast University, Nanjing 211189, People's Republic of China*

(Received 26 June 2018; accepted 22 August 2018; published online 18 September 2018)

Recently, an irreversible polymorphic transition from face-centered cubic to hexagonal close-packing was surprisingly observed under high pressure in the prototype CoCrFeMnNi high-entropy alloys (HEAs) by various research groups. This unexpected phase transition brings new insights into the stability of HEAs, and its irreversibility stimulates exploration for new HEAs via high-pressure compression synthesis. However, the onset pressure for the phase transition was reported to fluctuate over a vast range from ~7 to above 49 GPa in the reported experiments. The reason for this inconsistency remains unclear and puzzles the HEA community. To address this problem, this work systematically investigates the effects of non-hydrostaticity and grain size. Our results demonstrate that larger deviatoric stress induced by the non-hydrostaticity of the pressure medium and larger grain size of the initial sample can both promote a phase transition and, therefore, considerably depress the onset pressure. *Published by AIP Publishing.* https://doi.org/10.1063/1.5046180

Unlike the conventional alloys, which are based on one or two principal elements, high-entropy alloys (HEAs) usually contain five or more metallic elements with equimolar or near-equimolar ratios to maximize their configurational entropy.[1] Instead of forming typically expected composites with precipitation of various brittle intermetallic compounds, the complex compositions of HEAs can surprisingly stabilize single solid solution phases with a simple crystal structure, such as face-centered cubic (*fcc*), body-centered cubic (*bcc*), or hexagonal close-packed (*hcp*) structures. Over the last decade, HEAs have attracted intense research interest because of their unique combination of superior properties for broad potential applications, such as high ductility and strength in a wide temperature range, and excellent resistance to wear and corrosion.[2–5]

It is generally believed that HEAs possess high phase stability because of their high configurational entropy. In addition, their chemical complexity and packing disorder cause considerable local lattice distortion and sluggish atomic diffusion, which could further kinetically stabilize the systems.[4–6] These basic ideas about HEAs are supported by the observations of no polymorphic phase transition from cryogenic temperatures up to the melting temperatures in various HEAs over the last decade.[2,4] Recently, pressure-induced irreversible polymorphic transitions were discovered from *fcc* to *hcp* in the prototype *fcc* CoCrFeMnNi HEA at ~22 GPa[7–9] and also in another medium-entropy alloy system, NiCoCrFe alloy.[10] The *fcc* phase of the CoCrFeMnNi HEA was found to be stable at relatively high temperatures, while its *hcp* phase is more thermodynamically favorable at lower temperatures.[7] These results clarify the debate on the existence of the possibly more stable *hcp* phase at room temperature over the well-known *fcc* polymorph of the CoCrFeMnNi HEA. These polymorphic transitions are sluggish and irreversible; therefore, they open up an avenue of tailoring the structure and properties of HEAs.

However, Yu *et al.* compressed the CoCrFeMnNi HEA (prepared by mechanical alloying and high-pressure sintering with a grain size of ~100 nm) up to 31 GPa with silicone oil as the pressure medium, no phase transition was observed in *in situ* high-pressure XRD measurements.[11] Ahmad *et al.*,[12] studied the structure of CoCrFeMnNi HEA during compression up to ~49 GPa with neon as the pressure medium, again there was no phase transition. In another dynamic compression work on CoCrFeMnNi HEA by Jiang *et al.*, no phase transition was suggested below 11 GPa.[13] These previous studies by different research groups indicate that the onset pressure of the phase transition in the CoCrFeMnNi HEA fluctuates over a huge range from ~7 to above 49 GPa.[7–9,11–13] It is typically normal to have a small difference by a few percents in the starting pressures of a phase transition under different experimental conditions, and therefore, the large scattering of the onset pressures observed in the CoCrFeMnNi HEA in a relatively low-pressure region is surprising. The underlying reason remains unclear, which obstructs our

a)Authors to whom correspondence should be addressed: zengqs@hpstar.ac.cn and luzp@ustb.edu.cn.

understanding of the stability of HEAs and also the practical synthesis of the *hcp* phase and/or *hcp-fcc* dual-phase composites for applications. To address these issues, we carefully designed a series of *in situ* high-pressure x-ray diffraction experiments and studied the effect of non-hydrostaticity of the pressure environment on the phase transition by employing three different pressure mediums and the effect of grain size by loading different initial samples at the same time within one pressure chamber in a diamond anvil cell (DAC).

Regarding the pressure environment in a DAC, the stress tensor can be considered approximately symmetric with three nonzero components, one perpendicular (σ_3) to the diamond anvil surfaces and two coplanar ones (σ_1). The pressure (P) is equal to $(\sigma_3 + 2\sigma_1)/3$, and the deviatoric stress τ is equal to $\sigma_3 - \sigma_1$. Ideally, to accurately measure the equation of state (EOS) or the onset phase transition pressure of materials in compression experiments, the hydrostatic condition (i.e., the deviatoric stress $\tau = \sigma_3 - \sigma_1 = 0$) is required. In reality, the degree of hydrostaticity depends on how low the yield strength of the pressure medium is. In our previous study of the CoCrFeMnNi HEA, helium was used as the pressure transmitting medium.[7] Since helium is a very soft pressure medium, it is able to provide satisfactory hydrostatic pressure conditions up to 150 GPa.[14] In those positive experimental results, the onset pressure for the *fcc* to *hcp* transition was observed at ~22 GPa in helium.[7] In contrast, the transition was reported to start at a much lower pressure of ~14 GPa using silicone oil as the pressure medium by Tracy *et al.*[8] Silicone oil is regarded as a quasi-hydrostatic pressure medium above ~1 GPa.[15] Therefore, it is reasonable that the deviatoric (shear) stress gradually builds up above ~1 GPa in silicone oil, which could lower the onset pressure for the *fcc* to *hcp* transition. However, when a neon pressure medium was used, whose hydrostaticity is in-between helium and silicone oil, the onset pressure was reported to be ~7 GPa by Huang *et al.*,[9] thereby contradicting the trend found in other studies. To clarify this inconsistency, experiments must be performed on the same sample but only with different pressure mediums.

In situ high-pressure XRD experiments on the CoCrFeMnNi HEA samples were performed at beamline 12.2.2, at the Advanced Light Source (ALS), Lawrence Berkeley National Laboratory (LBNL) and also beamline 13-ID-D, at the Advanced Photon Source (APS), Argonne National Laboratory (ANL). The X-ray wavelengths were 0.4959 Å and 0.322 Å, respectively. DACs with a culet size of 400 μm were used to generate high pressure. The CoCrFeMnNi HEA samples were small spherical particles synthesized by gas-atomization (GA).[16] By selecting samples with nearly identical size, the difference in the grain size and thermal history between each sample was minimized to highlight the effect of the pressure mediums. A T301 stainless steel gasket was pre-indented to ~20 GPa, and then a hole was drilled inside the indentation as a sample chamber using a laser drilling system. The sample size was ~20 μm to avoid bridging the diamond anvils during compression (bridging anvils usually causes severe deviatoric stress on the sample). Two-dimensional XRD images were collected using two-dimensional area detectors and then integrated into a one-dimensional pattern using the Dioptas software.[17]

Figures 1(a), 1(b), and 1(c) present the XRD patterns of the same CoCrFeMnNi HEA samples collected with pressure

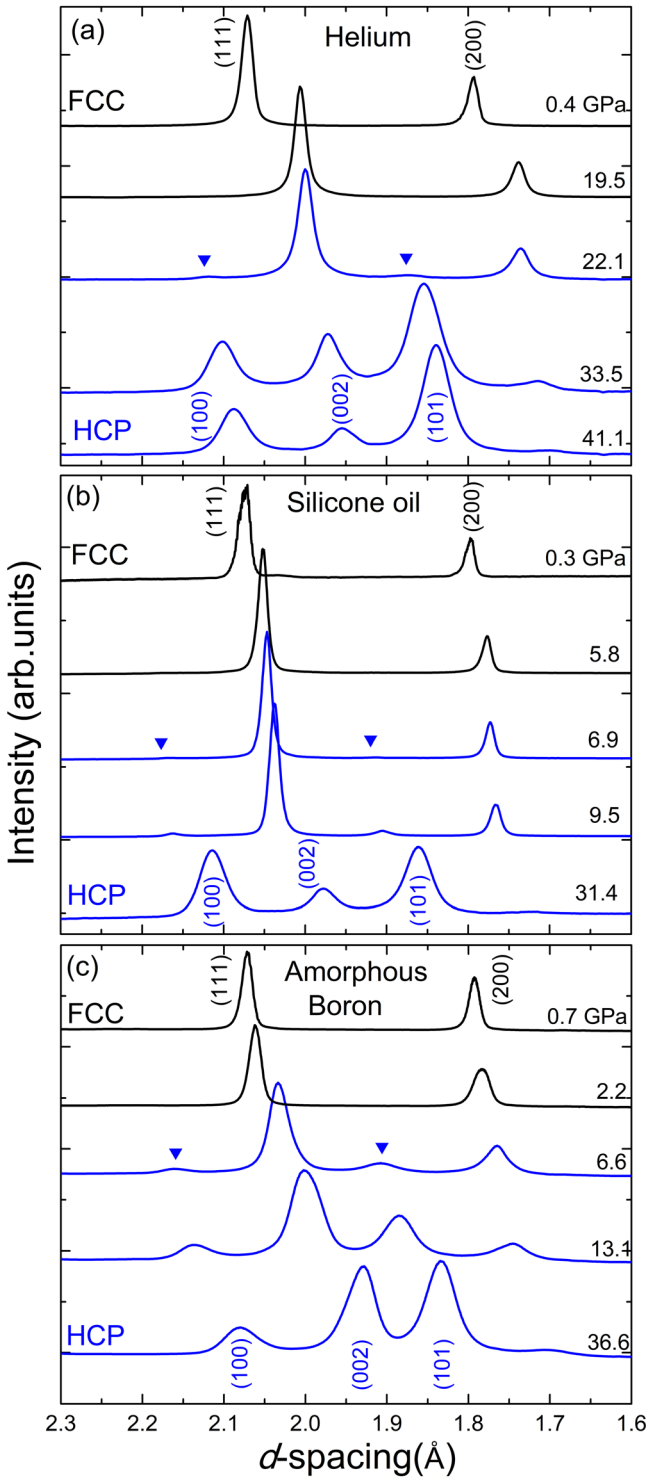

FIG. 1. XRD patterns of the CoCrFeMnNi HEA GA samples with helium[7] (a), silicone oil (b), and amorphous boron (c) as the pressure mediums during compression. The initial structure is *fcc*. All three samples gradually transform from *fcc* into *hcp* under high pressure. The onset pressures are determined as the *hcp* (100) and (101) peaks start to emerge, which are indicated by the blue triangles. Intensity mismatch to the standard *fcc* and *hcp* structures is mainly caused by relatively big grains of the initial samples or the texture developed during compression.

mediums of helium, silicone oil, and amorphous boron, respectively. The pressure was measured using the ruby fluorescence[18] and the EOS of the standard material Au.[19] According to the pressures that the *hcp* peaks start to emerge in the XRD patterns in Fig. 1, the onset transition pressure is estimated to be ~22 GPa in helium, ~7 GPa in silicone oil, and between 2 and 6 GPa in amorphous boron (there was too big a pressure step size to determine the exact onset pressure in amorphous boron). Amorphous boron is a super hard material [Mohs hardness: ~9.3 (Ref. 20)] and is typically used as a hard pressure medium to provide an extremely non-hydrostatic environment with low scattering background. Therefore, our experiments generated pressure environments with distinct hydrostaticity, i.e., the most hydrostatic (helium), the most non-hydrostatic (amorphous boron), and a quasi-hydrostatic condition in-between (silicone oil). It is clear that the onset pressure of the phase transition in the CoCrFeMnNi HEA shows a positive dependence on the hydrostaticity. Since the *fcc* to *hcp* transition in the CoCrFeMnNi HEA is suggested to have a sliding mechanism along the ⟨112⟩ direction on the {111} plane of the *fcc* phase, shear stress is a necessary driving force for sliding.[21] Therefore, it is reasonable that the deviatoric (shear) stress caused by the non-hydrostatic conditions could obviously promote the phase transition in the CoCrFeMnNi HEA. This observation is also consistent with the typical behaviors of the pressure-induced phase transition in many metals, such as iron[22] and titanium.[23]

Besides the effect of non-hydrostaticity as the critical external factor, in another experiment, we further studied the influence of internal grain size on the phase transition as a crucial internal factor in the initial samples. It is well known that during melt-quenching, grain growth can be effectively suppressed; a faster quenching rate gives rise to smaller average grain size. The GA process involves a high quenching rate, and as a result, relatively fine grains with an average size of ~5 μm can be obtained.[16] In contrast, the high-temperature annealed cast samples usually have low quenched-in strain but a large grain size above tens or hundreds of microns. A very spotty XRD pattern is generally obtained since the x-ray beam size for *in situ* high-pressure experiments is usually small, around 10 μm. Thus, in this work, rather than choosing the extensively studied cast CoCrFeMnNi HEA samples, we studied samples after high-pressure torsion (HPT) treatment. The HPT treatment enables us to reach the other extreme end of the grain size, down to ~10 nm.[24] The two samples with distinct grain size, obtained by GA and HPT, respectively, were loaded together into one symmetric DAC and located at equivalent positions to ensure identical pressure environments [indicated by the apexes of the triangle in Fig. 2(a)] in the sample chamber. Silicone oil was used as the pressure medium. Figure 2(b) shows the pressure gradient calculated by the pressure and position differences between the two ruby balls, which is a direct quantitative indicator of the degree of the non-hydrostaticity. Below ~2 GPa, it is almost ideally hydrostatic (the pressure difference between the two ruby balls are smaller than 0.1 GPa). Above ~2 GPa, the pressure gradient (deviatoric stress) firstly develops slowly, and then increases rapidly above 15 GPa. This trend is similar to the previous report of the hydrostaticity of silicone oil in a DAC.

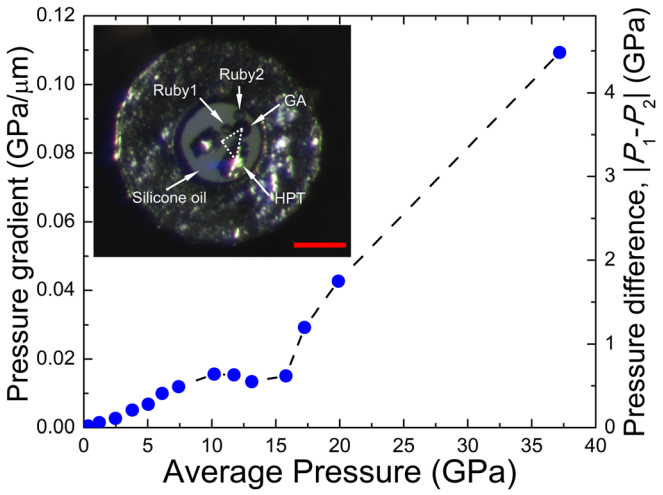

FIG. 2. The development of hydrostaticity in the sample chamber as a function of pressure. The inset shows the image of samples loaded in a DAC at 0.3 GPa. The GA and HPT samples were loaded together, along with two ruby balls as the pressure calibrant and silicone oil as the pressure medium. The spots of each sample for x-ray exposure are indicated by the two apexes of the triangle. The scale bar represents 100 μm. Two ruby balls were loaded into the sample chamber to quantitatively estimate the development of the pressure hydrostaticity. The distance between two ruby balls along the radial direction is $L \approx 41$ μm. The right Y-axis represents the pressure difference between the two ruby balls. The left-Y axis represents the pressure gradient which can be simply obtained ($\nabla P = |P_{\text{ruby1}} - P_{\text{ruby2}}|/L$) as an indicator of the pressure hydrostaticity. The average pressure is calculated as $P = (P_{\text{ruby1}} + P_{\text{ruby2}})/2$.

Figures 3(a) and 3(b) compare two-dimensional XRD images of the two samples loaded into the DAC at the initial pressure (0.3 GPa). The GA sample has a relatively spotty pattern with a grain size comparable to the x-ray beam size; however, the HPT sample has a very smooth pattern because

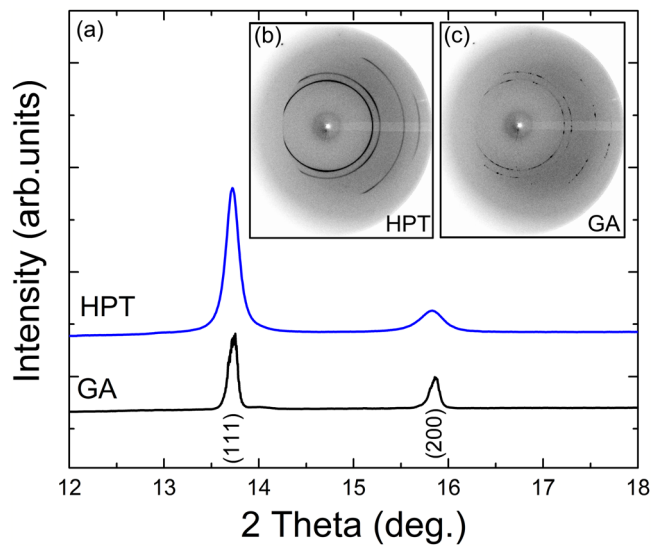

FIG. 3. Comparison of the XRD patterns of the GA and HPT samples loaded together in one DAC at the initial pressure of 0.3 GPa. (a) The integrated one-dimensional XRD patterns of the HPT and GA samples. (b) The smooth XRD image of the HPT sample and (c) the relatively spotty XRD image of the GA sample. The X-ray wavelength is 0.4959 Å. The peaks of the HPT sample are obviously broader than those of the GA sample due to the much smaller grain size. But there is no obvious peak position shift between the two samples.

of its tiny grains. Meanwhile, the small grain size of the HPT sample also results in a noticeable broadening of the diffraction peaks [Fig. 3(c)]. The almost identical XRD peak positions (e.g., $d_{111\_GA} = 2.076$ and $d_{111\_HPT} = 2.075$) reflects the negligible residual strain caused by the HPT treatment.

Figure 4 shows the XRD patterns of the GA and HPT samples as a function of pressure from 0.3 GPa all the way to the highest pressure of 31.4 GPa. Both transitions are sluggish, but their onset pressures are different. For the GA sample, the transition starts at 6.9 GPa, while the HPT specimen has a much higher onset pressure at ∼12.3 GPa (much larger than the pressure gradient level of ∼0.7 GPa). Since the spots of the two samples where the x-ray beam shot are equivalent in the pressure environment, the difference of the onset pressures should be attributed to the difference between the two samples themselves.

As previously discussed, the difference in the residual strain of the GA and HPT samples is negligible. It is usually

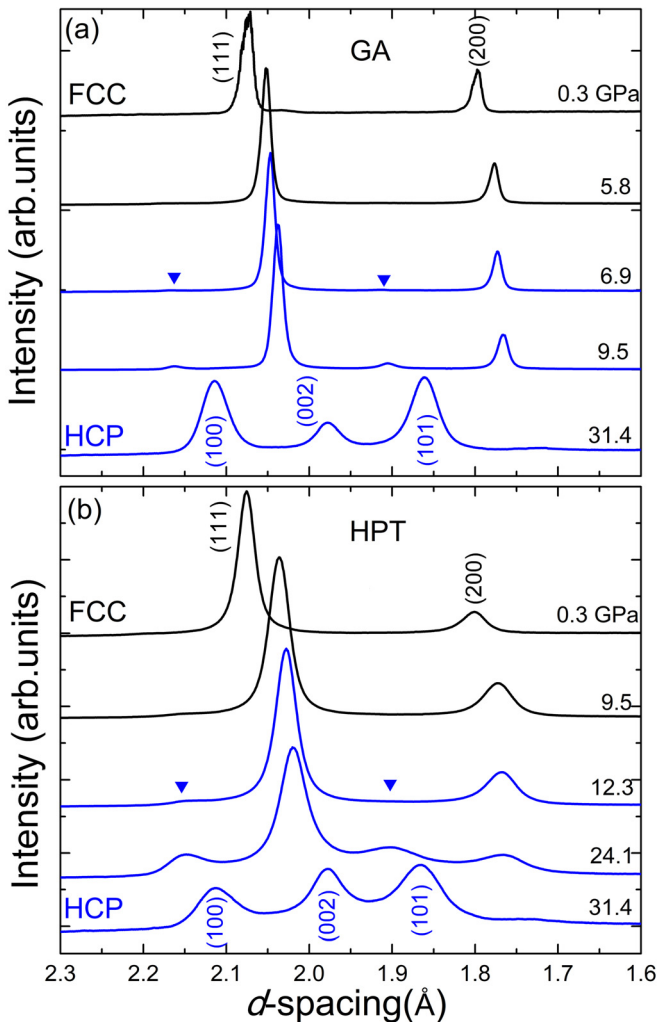

FIG. 4. XRD patterns of the CoCrFeMnNi HEA GA (a) and HPT (b) sample loaded together in one DAC with silicone oil as the pressure medium compressed from 0.3 up to 31.4 GPa. The GA sample has an onset pressure for the *fcc* to *hcp* transition of ∼6.9 GPa, while the HPT sample has a much higher onset pressure of ∼12.3 GPa. The initial structures are both *fcc*. Both samples gradually transform from an *fcc* into an *hcp* phase under high pressure. The onset pressures are determined where the *hcp* (100) and (101) peaks start to emerge, which are indicated by the blue triangles.

expected that the HPT sample may have a high density of dislocations after large shear deformation during its synthesis, which could affect the critical pressure for the *fcc* to *hcp* phase transition in the CoCrFeMnNi HEA. However, the previous study by Tang *et al*. on the mechanical properties of the HPT synthesized *fcc* HEAs found that the grain refinement (∼30 nm) plays a most crucial role for the hardness increment, while the contribution of the dislocation density to the hardness is almost negligible for the nanocrystalline alloy. This is evidenced by the fact that a reduction of ∼42% in the dislocation density after annealing gave no significant change in the hardness.[25] Moreover, in the case of the non-hydrostatic compression of CoCrFeMnNi HEA with amorphous boron as the pressure medium discussed before, the severe shear deformation and the resultant high density of dislocation did not enhance but significantly decrease the transition pressure down to ∼6 GPa. Therefore, the significantly increased onset pressure of the HPT sample should be mainly attributed to the grain size effect, i.e., the smaller the grain size, the higher the onset transition pressure. A similar grain size effect on high pressure-induced phase transitions in semiconductor nanocrystals, such as Si, CdSe, CdS,[26] and ZnO,[27] has been extensively observed. The underlying mechanism is believed to be associated with the significant increment of the grain interface energy of the high-pressure phase nuclei once the grain size of the starting material decreases down to the nanoscale. However, in the multicomponent HEAs, the circumstance may be much more complicated than that in traditional materials with simple compositions,[28] the details of the mechanism of the grain size effect on the transition pressure calls for exploration in the future study.

In summary, by using different pressure mediums in the *in situ* high-pressure XRD experiments on the GA samples, the *fcc*-to-*hcp* transition in the CoCrFeMnNi HEA was found to be extremely sensitive to the hydrostaticity. Specifically, the deviatoric stress induced by non-hydrostaticity of the pressure medium can obviously prompt the transition. As a result, the onset pressure does drop from ∼22 to ∼2–6 GPa when the pressure medium is changed from helium to amorphous boron. Moreover, in another experiment with two different samples loaded in one DAC, it was demonstrated that the grain size also plays a vital role, i.e., the smaller the grain size, the higher the onset transition pressure. Therefore, it is suggested that the inconsistency of the reported onset pressure of the *fcc*-to-*hcp* transition in the CoCrFeMnNi HEA by different groups may be caused by the different hydrostaticity induced by different pressure mediums and/or the bridging between the sample and anvils under high pressure, also the difference in grain sizes of the initial samples. Our result clarifies the debate regarding the onset pressure of the *fcc*-to-*hcp* transition in the CoCrFeMnNi HEA, which will deepen our understanding of the stability of the HEAs. Moreover, the external and interior effects on the transition revealed in this work could facilitate the synthesis of the new *hcp* or *hcp*/*fcc* dual phase CoCrFeMnNi HEA composite for fundamental study or practical applications.

This research was supported by the National Thousand Youth Talents Program in China, the National Natural

Science Foundation of China (Nos. 51871054, U1530402, 51671018, 11790293, 51531001, 51422101, 51371003, and 51671021), the 111 Project (B07003), the International S&T Cooperation Program of China (2015DFG52600), and the Program for Changjiang Scholars and Innovative Research Team in University (IRT_14R05). We would like to thank Dr. Hamed Shahmir for the HPT sample synthesis, Dr. Sergey N. Tkachev for his help with the gas loading at GeoSoilEnviroCARS (GSECARS), and Freyja O'Toole for editing the manuscript. The XRD experiment was carried out at the beamline 12.2.2, Advanced Light Source (ALS). ALS was supported by the Director, Office of Science, DOE-BES under Contract No. DE-AC02-05CH11231. Portions of the XRD experiment were carried out at the beamline GSECARS-ID-D. GSECARS was supported by the National Science Foundation (NSF)-Earth Sciences (EAR-1128799) and Department of Energy (DOE)-GeoSciences (DE-FG02-94ER14466). The use of the gas loading system at sector 13 was supported by COMPRES (EAR 11-57758), NSF (EAR-1128799), and DOE (DE-FG02-94ER14466). APS was supported by the DOE Office of Science (DE-AC02-06CH11357).

[1]J. W. Yeh, S. K. Chen, S. J. Lin, J. Y. Gan, T. S. Chin, T. T. Shun, C. H. Tsau, and S. Y. Chang, Adv. Eng. Mater. **6**, 299 (2004); Y. Zhang, T. T. Zuo, Z. Tang, M. C. Gao, K. A. Dahmen, P. K. Liaw, and Z. P. Lu, Prog. Mater. Sci. **61**, 1 (2014); Y. F. Ye, Q. Wang, J. Lu, C. T. Liu, and Y. Yang, Mater. Today **19**, 349 (2016).

[2]F. Otto, A. Dlouhy, C. Somsen, H. Bei, G. Eggeler, and E. P. George, Acta Mater. **61**, 5743 (2013); B. Gludovatz, A. Hohenwarter, D. Catoor, E. H. Chang, E. P. George, and R. O. Ritchie, Science **345**, 1153 (2014).

[3]S. Praveen and H. S. Kim, Adv. Eng. Mater. **20**, 1700645 (2018); N. Stepanov, M. Tikhonovsky, N. Yurchenko, D. Zyabkin, M. Klimova, S. Zherebtsov, A. Efimov, and G. Salishchev, Intermetallics **59**, 8 (2015); Y. Zou, H. Ma, and R. Spolenak, Nat. Commun. **6**, 7748 (2015); Z. J. Zhang, M. M. Mao, J. W. Wang, B. Gludovatz, Z. Zhang, S. X. Mao, E. P. George, Q. Yu, and R. O. Ritchie, *ibid.* **6**, 10143 (2015); O. N. Senkov, G. B. Wilks, J. M. Scott, and D. B. Miracle, Intermetallics **19**, 698 (2011); M. H. Chuang, M. H. Tsai, W. R. Wang, S. J. Lin, and J. W. Yeh, Acta Mater. **59**, 6308 (2011); Y. Z. Shi, B. Yang, X. Xie, J. Brechtl, K. A. Dahmen, and P. K. Liaw, Corros. Sci. **119**, 33 (2017); D. B. Miracle and O. N. Senkov, Acta Mater. **122**, 448 (2017).

[4]W. H. Liu, Y. Wu, J. Y. He, T. G. Nieh, and Z. P. Lu, Scr. Mater. **68**, 526 (2013).

[5]K. Y. Tsai, M. H. Tsai, and J. W. Yeh, Acta Mater. **61**, 4887 (2013).

[6]Z. J. Wang, Y. H. Huang, Y. Yang, J. C. Wang, and C. T. Liu, Scr. Mater. **94**, 28 (2015).

[7]F. Zhang, Y. Wu, H. B. Lou, Z. D. Zeng, V. B. Prakapenka, E. Greenberg, Y. Ren, J. Y. Yan, J. S. Okasinski, X. J. Liu, Y. Liu, Q. S. Zeng, and Z. P. Lu, Nat. Commun. **8**, 15687 (2017).

[8]C. L. Tracy, S. Park, D. R. Rittman, S. J. Zinkle, H. B. Bei, M. Lang, R. C. Ewing, and W. L. Mao, Nat. Commun. **8**, 15634 (2017).

[9]E. W. Huang, C. M. Lin, J. Jain, S. R. Shieh, C. P. Wang, Y. C. Chuang, Y.-F. Liao, D. Z. Zhang, T. Huang, T. N. Lam, W. Woo, and S. Y. Lee, Mater. Today Commun. **14**, 10 (2018).

[10]F. X. Zhang, S. J. Zhao, K. Jin, H. B. Bei, D. Popov, C. Y. Park, J. C. Neuefeind, W. J. Weber, and Y. W. Zhang, Appl. Phys. Lett. **110**, 011902 (2017).

[11]P. F. Yu, L. J. Zhang, H. Cheng, H. Zhang, M. Z. Ma, Y. C. Li, G. Li, P. K. Liaw, and R. P. Liu, Intermetallics **70**, 82 (2016).

[12]A. S. Ahmad, Y. Su, S. Y. Liu, K. Ståhl, Y. D. Wu, X. D. Hui, U. Ruett, O. Gutowski, K. Glazyrin, H. P. Liermann, H. Franz, H. Wang, X. D. Wang, Q. P. Cao, D. X. Zhang, and J. Z. Jiang, J. Appl. Phys. **121**, 235901 (2017).

[13]Z. J. Jiang, J. Y. He, H. Y. Wang, H. S. Zhang, Z. P. Lu, and L. H. Dai, Mater. Res. Lett. **4**, 226 (2016).

[14]A. Dewaele and P. Loubeyre, High Pressure Res. **27**, 419 (2007).

[15]S. Klotz, J. C. Chervin, P. Munsch, and G. L. Marchand, J. Phys. D Appl. Phys. **42**, 075413 (2009); R. J. Angel, M. Bujak, J. Zhao, G. D. Gatta, and S. D. Jacobsen, J. Appl. Cryst. **40**, 26 (2007).

[16]Y. Liu, J. S. Wang, Q. H. Fang, B. Liu, Y. Wu, and S. Q. Chen, Intermetallics **68**, 16 (2016).

[17]C. Prescher and V. B. Prakapenka, High Pressure Res. **35**, 223 (2015).

[18]H. K. Mao, J. Xu, and P. M. Bell, J. Geophys. Res.-Solid Earth **91**, 4673, https://doi.org/10.1029/JB091iB05p04673 (1986).

[19]Y. W. Fei, A. Ricolleau, M. Frank, K. Mibe, G. Y. Shen, and V. B. Prakapenka, Proc. Natl. Acad. Sci. **104**, 9182 (2007).

[20]G. V. Samsonov, in *Handbook of the Physicochemical Properties of the Elements*, edited by G. V. Samsonov (Springer US, Boston, MA, 1968), p. 432.

[21]Y. Akahama, M. Nishimura, K. Kinoshita, H. Kawamura, and Y. Ohishi, Phys. Rev. Lett. **96**, 045505 (2006).

[22]N. V. Barge and R. Boehler, High Pressure Res. **6**, 133 (1990).

[23]D. Errandonea, Y. Meng, M. Somayazulu, and D. Häusermann, Physica B **355**, 116 (2005).

[24]H. Shahmir, J. Y. He, Z. P. Lu, M. Kawasaki, and T. G. Langdon, Mater. Sci. Eng. A **676**, 294 (2016).

[25]Q. H. Tang, Y. Huang, Y. Y. Huang, X. Z. Liao, T. G. Langdon, and P. Q. Dai, Mater. Lett. **151**, 126 (2015).

[26]S. H. Tolbert and A. P. Alivisatos, Ann. Rev. Phys. Chem. **46**, 595 (1995).

[27]L. Bayarjargal, L. Wiehl, and B. Winkler, High Pressure Res. **33**, 642 (2013).

[28]D. Ma, B. Grabowski, F. Körmann, J. Neugebauer, and D. Raabe, Acta Mater. **100**, 90 (2015).